

Soft modes in RADP dipole glass

A. A. Volkov, G. V. Kozlov, S. P. Lebedev, A. V. Sinitskii, S. Kamba,¹⁾ and J. Petzelt¹⁾

Institute of General Physics, USSR Academy of Sciences

(Submitted 18 June 1991)

Zh. Eksp. Teor. Fiz. **101**, 248–255 (January 1992)

Submillimeter and infrared spectroscopy are used to obtain the dielectric-response function of a mixed rubidium-ammonium-dihydrophosphate crystal in the frequency range 8–650 cm^{-1} at temperatures 5–300 K. Collective proton soft modes, similar to those observed in pure rubidium and ammonium dihydrophosphates, were recorded in the para-phase. Their temperature evolution and their transformation into still lower excitations typical of the dipole-glass phase were tracked. The phenomenon is interpreted as a transformation of a ferroelectric soft mode into a central peak, so that the state of dipole glass can be represented as the result of an incomplete ferroelectric phase transition.

INTRODUCTION

A model object intensively investigated, in view of the increased interest in disordered states of solids, is the compound RADP, a solid solution of the crystals RbH_2PO_4 (RDP) and $(\text{NH}_4)\text{H}_2\text{PO}_4$ (ADP) belonging to the known family of crystals with hydrogen bonds, of the potassium diphosphate (KDP) type.¹ The RDP–ADP combination is unique because the lattice constants of RDP and ADP are almost equal, since the radii of the Rb^+ ion and the NH_4^+ complex are close in value. This makes it possible to grow high-quality large crystals of the solid solution $\text{Rb}_{1-x}(\text{NH}_4)_x\text{H}_2\text{PO}_4$ with arbitrary relative concentration $0 \leq x \leq 1$. At the same time, the different manners in which Rb^+ and NH_4^+ interact with their environments produce in the RDP and ADP crystals different phase transitions, ferroelectric ($T_c = 146$ K) and antiferroelectric ($T_c = 148$ K) respectively. The mixed RADP crystal also undergoes corresponding phase transitions at $x < 0.23$ and $x > 0.74$, but in the compounds produced at intermediate densities the phase transition is suppressed by the competition between differently directed types of ordering, and at low temperatures a state of dipole glass evolves (without abrupt anomalies) in place of one of the ordered phases. The attributes of such a state are revealed by an aggregate of anomalies manifested by the temperature dependences of the lattice parameters,² the speed of sound,³ birefringence,⁴ and dielectric constants.⁵

To observe the lattice excitations corresponding to the dynamics of the vitreous phase, many spectroscopic investigations were made using dielectric measurements,⁶ light scattering,^{7,8} and neutron scattering.⁹ An onset of strong dielectric losses at radio and microwave frequencies were observed¹⁰ in the transition of RADP into the vitreous phase. The absorption is very strongly smeared out over the spectrum in the 10^5 – 10^{10} Hz range and has a strongly pronounced temperature dependence. Attempts to analyze the loss spectrum, using simple dispersion models based on the Debye relaxation model, yield consistently a broad relaxation-time distribution whose microscopic meaning is not fully clear.¹¹ It appears that this approach to the interpretation of the loss spectrum is too formal, and it seems to us that the question of the origin of low-frequency relaxation in RADP must be answered from a general standpoint.

We analyze here the dielectric-response function of RADP in a greatly extended range of frequencies and tem-

peratures, including, in addition to the radio and microwave bands, also the submillimeter and infrared bands. Our purpose is to connect the onset of low-frequency relaxation with the temperature properties of the dielectric-response function at high frequencies.

2. EXPERIMENT

Our experimental data pertain to RADP with relative concentration $x = 0.5$. The measurements were performed with the electric-field vector \mathbf{E} perpendicular and parallel to the tetragonal axis c of the paraphase, i.e., we investigated the polar excitations in the hydrogen-bond plane and in the plane perpendicular to it. The dielectric-response function was determined from the results of submillimeter (8–18 cm^{-1}) measurements with “Epsilon” backward-wave-tube laboratory spectrometer,¹² and the IR data obtained with the “Brooker” IFS-113v Fourier spectrometer (30–650 cm^{-1}). In the former case we measured the complex transmission coefficients of plane-parallel specimens, and in the latter the spectra of reflection from an “infinite layer.” The real and imaginary parts $\epsilon'(\nu)$ and $\epsilon''(\nu)$ of the dielectric constant in the submillimeter band were directly recalculated from the experimental data using the plane-layer equations, while the infrared $\epsilon'(\nu)$ and $\epsilon''(\nu)$ spectra were obtained by reducing the reflection spectra by the Kramers–Kronig equations using submillimeter data for reconciliation at low frequencies. The dielectric spectra obtained in this manner are shown in Fig. 1.

3. DISCUSSION OF EXPERIMENTAL RESULTS

A characteristic property of the RADP dielectric-response functions is the presence, at both orientations, of a strong temperature-dependent dispersion in the 10–100 cm^{-1} range. This dispersion produces a strong diffuse background, on which it is possible to observe approximately above 100 cm^{-1} a set of resonant phonon peaks. A direct comparison of the RADP spectra with the spectra of pure RDP and ADP shows them to be qualitatively similar (Fig. 2).^{13,14} This allows us to state that, just as in pure RDP and ADP, the broad dispersion of $\epsilon'(\nu)$ and $\epsilon''(\nu)$ in the 10–100 cm^{-1} interval is due mainly to proton dynamics. It is particularly interesting and important that in the case of RADP the evolution of the proton-subsystem response with temperature is not interrupted by abrupt phase transitions, but

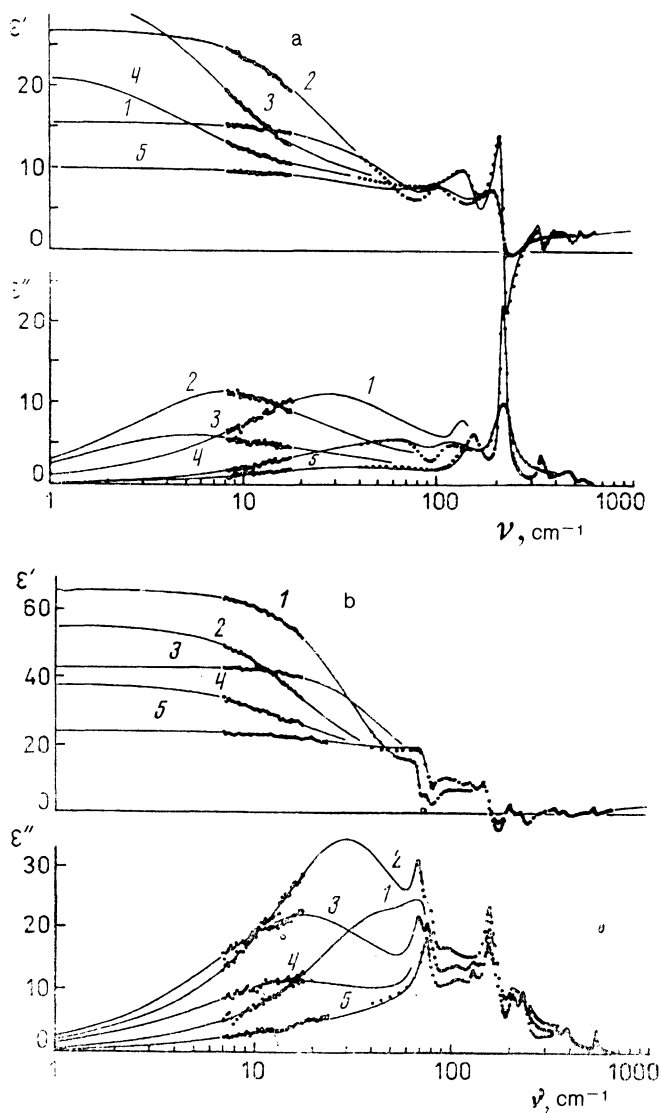


FIG. 1. Dielectric spectra $\epsilon'(\nu)$ and $\epsilon''(\nu)$ of RADP dipole glass in orientations $E\parallel c$ (a) and $E\perp c$ (b) at temperatures (T , K) 1—275, 2—108, 3—53, 4—35, 5—5. Points in the region $\nu \sim 10 \text{ cm}^{-1}$ —submillimeter backward wave tube spectroscopy data, above 40 cm^{-1} —calculated using the Kramers–Kronig equations from IR reflection spectra. Solid lines—model of independent oscillators.

continues monotonically down to the lowest temperatures at which the dipole-glass state sets in.

Figure 3 (Refs. 15 and 16) shows the qualitative temperature dependences of proton modes whose parameters were obtained from a dispersion analysis of the $\epsilon'(\nu)$ and

$\epsilon''(\nu)$ spectra by least squares in the framework of the additive multi-oscillator model. These parameters are in accord with the results of the model calculations shown by solid curves in Fig. 1. The strong slowing of the proton modes prevents an unambiguous separation in the model oscillators, of the width and frequency, which are therefore shown in Fig. 3 in terms of the $\nu_0 = 1/2\pi\tau$ relaxation model, corresponding simply to the frequencies of the absorption-line maxima. To describe the broad dispersion band in both orientations it was necessary to use at least two overdamped oscillators, since it can be seen even in rough approximation that the low- and high-frequency parts of the background behave quite differently: the former vanishes at low frequency, and the latter ($\nu > 50 \text{ cm}^{-1}$) remains practically untouched. At 5 K there remains in the spectrum a broad absorption band (relaxator) with a maximum near 90 cm^{-1} , and while its amplitude is low in the polarization $E\parallel c$, it is appreciable at $E\perp c$ and influences the entire form of the spectrum. A similar background is observed also in the optical Raman scattering spectrum.⁷ Obviously, this temperature-independent polarization mechanism can be regarded as autonomous. In our simple additive model we treat it as a separate term and do not show it in Fig. 3.

In the $E\parallel c$ orientation, at the RDP and ADP paraphase temperatures, the proton mode in RADP looks like a simple superposition of coexisting excitations in RDP and ADP (Fig. 3), having a symmetry B_{2u} . The oscillations of this symmetry correspond to a proton ordering in the ab plane causing formation of a dipole moment along the c axis. In RDP and ADP this polarization mechanism is temperature-unstable, and the frequency of the B_{2u} oscillations decreases with temperature. In RDP, in final analysis, it practically vanishes at the point of the ferroelectric phase transition at $T = 146 \text{ K}$ (Fig. 3). In ADP the temperature dependence of the frequency of the B_{2u} mode also attests to some tendency of the lattice to become ferroelectrically ordered, but at $T = 148 \text{ K}$ there vanishes in ADP the frequency of an entirely different mode located at the boundary of the Brillouin zone and therefore inactive in the dielectric and IR spectra. It causes the antiferroelectric phase transition in ADP.

In the $E\perp c$ orientation, the proton mode in RADP hardly differs, with respect to its manifestation in the spectra at high temperatures, from the known pure ADP and RADP E -symmetry modes corresponding to polar ordering of the protons themselves on the hydrogen bonds in the ab plane.

We conclude thus that the same processes of ordering and disordering the proton subsystem, which determine the dynamics of the initially pure crystals (the B_{2u} and E

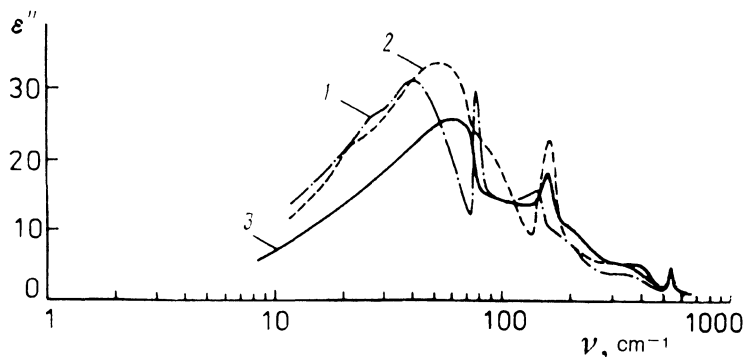


FIG. 2. Comparison of $\epsilon''(\nu)$ spectra, for $E\perp c$, of pure RDP (1) and ADP (2) crystals^{13,14} and of mixed RADP (3) (see Fig. 1b).

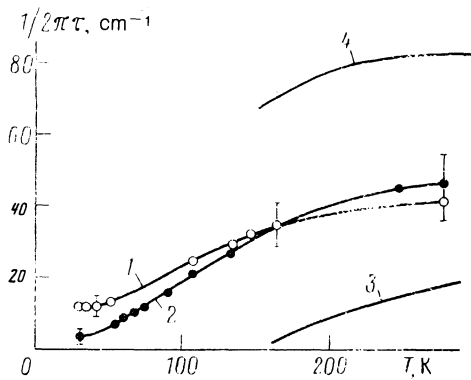


FIG. 3. Temperature dependences of frequencies of polar phonon modes in the mixed crystal RADP (1—E \perp c, 2—E \parallel c) and pure RDP (3, E \parallel c) and ADP (4, E \perp c).^{15,16}

modes), dominate at paraphase temperatures in the RADP solid solution. Now, however, these processes can be tracked in RADP at temperatures heretofore inaccessible on account of the transitions of RDP and ADP into an ordered state. As seen from Fig. 3, the proton modes in RADP are monotonically softened when the temperature is lowered.

In the E \parallel c polarization, the mode frequency reaches 3 cm⁻¹, and in the other polarization the mode softens only to 10 cm⁻¹. To a temperature on the order of 100 K, the dielectric mode follow up strictly the temperature behavior of the static dielectric constant (Fig. 4),^{17,18} showing that no lower-frequency modes exist in the crystal.

At $T < 100$ K, when vitrification starts, the changes no longer follow the variation of $\epsilon_0(T)$. The oscillator strengths of the modes $f = \Delta\epsilon/2\pi\tau$ drop abruptly (Fig. 5), thus indicating unambiguously that the soft-mode charges become redistributed into lower-frequency excitations. The latter are precisely the ones observed at radio frequencies and represent the dynamics of the vitreous phase.

From the phenomenological standpoint, the described process is none other than a transfer of the ferroelectric soft mode into the central peak. This phenomenon is well known for many structural phase transitions and evolves as a rule in a narrow temperature interval in the immediate vicinity of T_c . The behavior of the RADP spectra gives grounds for suggesting that RADP is also in a state of a phase transition that spans a temperature range of about 150 degrees and is not completed even at liquid-helium temperature.

One of the fruitful approaches to the interpretation of such phenomena in smeared-out phase transitions is the cluster concept.¹⁹ The main idea is that as T_c is approached

advance clusters of the new phase are produced. The soft-mode phonons are transformed into intracluster oscillations, and the much slower motion of the cluster boundaries develops into a low-frequency central peak. These two types of motion correspond to two substantially different relaxation times.

Our analogy between the critical dynamics in a phase transition and the dynamics of a vitreous phase presupposes that RADP contains formations corresponding to pretransition clusters. Actually, investigations by methods of molecular dynamics,²⁰ x-ray scattering,²¹ and neutron scattering²² indicate that the dipolar glass RADP contains regions of spatial correlations of average scale (over a distance of several lattice constants). The presence of two time scales attests to the breakup of the system into two spatially separated components with different relaxation times.

According to diffuse neutron-scattering data, the wave vector of the correlations corresponding to clusters is not commensurate with the lattice period, and the characteristic correlation length in the ab plane reaches 20 Å at 100 K and stops growing with further cooling.²²

The onset of such incommensurate correlations of average scale is in our opinion exceedingly important, since it makes it possible to relate in principle the "strong disorder" in a vitreous phase with "disorder" in an incommensurate phase. It is not excluded that a superposition of only several incommensurabilities generates externally a state so complicated that it is difficult to discern in it any disorder, and is therefore describable as a "vitreous phase."

With the aid of incommensurate correlations one can explain also the diffuse loss background observed at E \perp c (Fig. 2), which is independent of temperature and is preserved in the vitreous phase. It is known that in a structure of the KDP type the energywise most favorable situation is one in which two protons are located near each PO₄ tetrahedron (the Slater rule). The existence of regions with different degrees of ordering causes this rule to be violated: polar HPO₄ — H₃PO₄ pairs (Takaga defects²³) with proton shortage and excess are formed on the cluster boundaries. It seems to us that the oscillations of the charged boundaries interact with the acoustic oscillation mode, forming a micropiezoresonant mode of sorts, which is observed in the IR spectrum (Fig. 6). In other words, the density of the acoustic-mode phonon states becomes IR-active. Its temperature stability is due to the fact that below 100 K the correlation wave vector is independent of temperature. Assuming the characteristic frequency of the ν_0 mode to be 90 cm⁻¹ and substituting the sound velocity $V_L = 4100$ m/s obtained by us from Man-

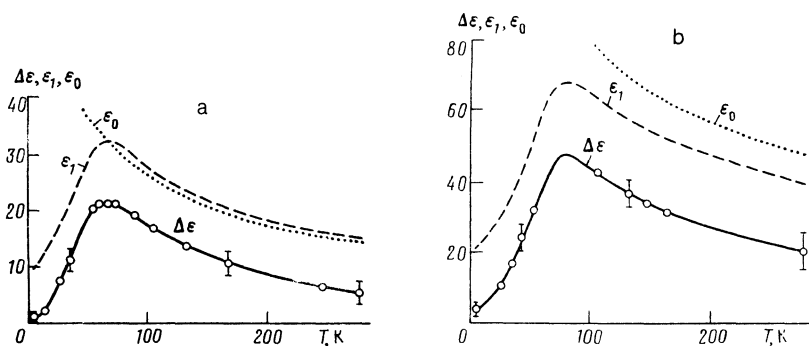


FIG. 4. Temperature dependences of dielectric contribution $\Delta\epsilon$ of the soft mode of the dielectric constant ϵ_1 at the frequency ~ 1 cm⁻¹ and of the static ϵ_0 (Refs. 17, 18) in polarizations E \parallel c (a) and E \perp c (b).

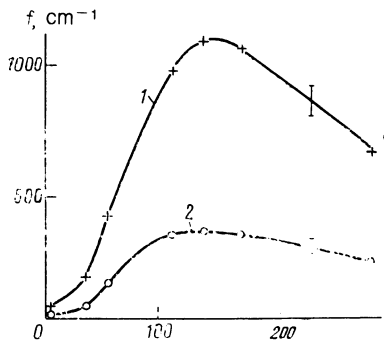


FIG. 5. Temperature dependences of soft-mode oscillator strengths 1— $E_{\perp}c$, 2— $E_{\parallel}c$.

del'shtam-Brillouin scattering data⁸ we obtain for the correlation length

$$\lambda = \frac{1}{k} = \frac{\text{tg } \alpha}{v_0} = \frac{V_L}{v_0} \approx 15 \text{ \AA}.$$

The corresponding value for a deuterated sample is 20 Å according to neutron-investigation data.²²

4. CONCLUSION

The analysis of the RADP, dielectric response has been extended from the radio and microwave frequencies to the submillimeter and infrared wavelength band, and has made possible a direct comparison of the dielectric spectra of RADP and pure RDP and ADP under disordered-paraphase conditions. It is concluded from the similarity of the spectra that, just as in pure RDP and ADP, the high-temperature dynamics of RADP is determined by B_{2u} - and E -symmetry ordering. Since phase transitions occurring in pure RDP and ADP are suppressed in RADP, the temperature behavior of the B_{2u} and E modes in RADP can be tracked down to the lowest temperature. A steep decrease of the oscillator strengths of these modes has been observed in the vitreous phase and attests to a redistribution of the charges of the B_{2u} and E modes into low-frequency (radio and microwave) excitations previously observed and related to the dynamics of dipole glass.

In a variant proposed for the analysis of the dynamic picture in RADP, the transition into the dipole-glass state is represented as ferroelectric phase transition extended over a large temperature region and not completed even at liquid-helium temperature. The picture of the dielectric spectrum is described qualitatively assuming a cluster dynamics that determines the microscopic dynamics of the dipole-glass phase.

An estimate of the characteristic dimension of the clusters, $\sim 15 \text{ \AA}$, has been obtained from the frequency of the temperature-independent IR mode.

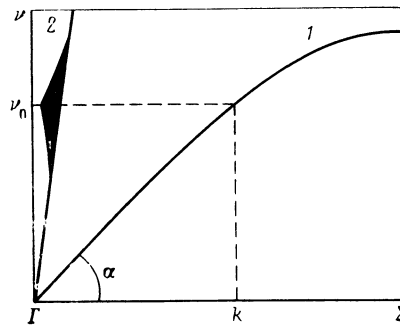


FIG. 6. Scheme of interaction between cluster-structure oscillations with wave vector k and acoustic oscillations; and Σ are the center and boundary of the Brillouin zone; 1—acoustic mode, α —inclination angle (speed of sound); 1—IR-active mode.

The approach proposed relates qualitatively, for the first time ever, the dynamic phenomena in the dipole-glass phase with the critical dynamics in a ferroelectric phase transition.

The authors thank H. Schmidt for supplying the specimens and for initiative in launching the research, and A. I. Ritus for help with the analysis of the Brillouin-scattering data.

¹¹Physics Institute, Czechoslovak Academy of Sciences, Prague.

¹²E. Courtens, *Helv. Phys. Acta* **56**, 705 (1983).

¹³E. Courtens, T. F. Rosenbaum, S. E. Nagler, and P. M. Horn, *Phys. Rev. B* **29**, 515 (1984).

¹⁴E. Courtens and R. Vacher, *Phys. Rev. B* **35**, 7271 (1987).

¹⁵E. Courtens, E. Vacher, and Y. Dagorn, *ibid.* **36**, 318 (1987).

¹⁶E. Courtens, *ibid.* **33**, 2975 (1986).

¹⁷A. Sammara and H. Terauchi, *Phys. Rev. Lett.* **59**, 347 (1987).

¹⁸E. Courtens and H. Vogt, *Z. Phys. B* **62**, 143 (1986).

¹⁹E. Courtens, R. Vacher, and Y. Dagorn, *Phys. Rev. B* **33**, 7625 (1986).

²⁰E. Courtens, R. A. Cowley, and H. Grimm, *Ferroelectrics* **78**, 275 (1988).

²¹H. J. Brucner, E. Courtens, and H.-G. Unruh, *Z. Phys. B* **73**, 337 (1988).

²²R. H. Cole, *Ann. Rev. Phys. Chem.* **40**, 1 (1989).

²³A. A. Volkov, Yu. G. Goncharov, G. V. Kozlov, and S. P. Lebedev, *Elektron. Tekhn. Ser 1*, No. 11, 38 (1984).

²⁴P. Simon, F. Grevais, and E. Courtens, *Phys. Rev. B* **37**, 3969 (1988).

²⁵T. Kawamura and A. Mitsuishi, *Technology Reports of the Osaka University*, 23, No. 1123, 365 (1973).

²⁶A. A. Volkov, G. V. Kozlov, S. P. Lebedev, and A. M. Prokhorov, *Ferroelectrics* **25**, 531 (1980).

²⁷A. A. Volkov, G. V. Kozlov, S. P. Lebedev, and A. M. Prokhorov, *J. Phys. Soc. Jpn.* **49**, Suppl. B, 188 (1985).

²⁸V. H. Schmidt, Z. Trybula, D. He *et al.*, *Ferroelectrics* **106**, 119 (1990).

²⁹S. Iida and H. Terauchi, *J. Phys. Soc. Jpn.* **52**, 4044 (1983).

³⁰A. D. Bruce and R. A. Cowley, *Structural Phase Transition*, Taylor and Francis (1981).

³¹K. Parlinski and H. Grimm, *Phys. Rev. B* **37**, 1925 (1988).

³²E. Courtens, R. A. Cowley, and A. Grimm, *Ferroelectrics* **78**, 275 (1988).

³³H. Grimm, in *Dynamics of Disordered Materials*, Springer, 1989, p. 274.

³⁴Y. Takagi, *J. Phys. Soc. Jpn.* **3**, 273 (1948).

Translated by J. G. Adashko